Iranian Journal of Chemical Engineering

Journal Homepage: www.ijche.com

pISSN: 1735-5397
eISSN: 2008-2355

Full Paper

Modeling and Simulation of the Magnetorheological Fluid Sleeve Valve

A. E. Pourshayan [1], A. Rabbani [2], S. Farahani [3], Y. Rabbani [2,4*], H. Ahmadi Danesh Ashtiani [1], M. Shariat [4], M. Gholi Nejad [5], A. A. Emami Satloo [6]

[1] Department of Mechanical Engineering, South Tehran Branch, Islamic Azad University, Tehran, Iran
[2] School of Chemical Engineering, College of Engineering, University of Tehran, P. O. Box: 111554563, Tehran, Iran
[3] School of Chemical Engineering, Iran University of Science and Technology, Tehran, Iran
[4] PetroPars Operation and Management Company (POMC), Tehran, Iran
[5] Research and Technology Directorate, National Iranian Gas Company, Alborz Province Gas Company, Karaj, Iran
[6] Metering Senior Engineering, National Iranian Gas Company, Alborz Province Gas Company, Karaj, Iran

ARTICLE INFO

Article history:
Received: 2021-03-01
Accepted: 2021-05-31
Available online: 2021-11-02

Keywords:
Magnetorheological Fluid,
Magnetorheological Valve,
Rheology,
Magnetic Field,
Pressure

ABSTRACT

Magnetorheological fluids contain suspended magnetic particles that arrange in chains in the presence of a magnetic field, causing the conversion of the fluid from a liquid state to a quasi-solid state. These fluids can be used in valves as a tool for pressure drop and flow interruption. This research aims to investigate the feasibility of using the magnetorheological fluid (MRF) in industrial valves. The rheological properties of the MRF sample were measured with the MCR300 rheometer in the presence of a magnetic field. In this connection, the Bingham plastic continuous model was used to predict the fluid behavior, and the model coefficients were obtained using MATLAB software. Then, the model coefficients were used to simulate the behavior of the magnetorheological fluid in the presence of the magnetic field in the valve. The geometry and dimensions of the valve were designed according to the dimensions of industrial samples. Then the CFD simulation with Fluent software was done by using the Bingham model and fluid characteristics obtained from experimental results. The results showed that the pressure increased by increasing the magnetic field at the center of the sleeve. The magnetic field of up to 0.5 Tesla, increases pressure and decreases amplitude. Therefore, as the magnetic field increased, the amplitude of the maximum pressure on the sleeve was significantly reduced.

DOI: 10.22034/ijche.2021.131248 URL: http://www.ijche.com/article_131248.html

*Corresponding author: yahyarabbani@ut.ac.ir (Y. Rabbani)

1. Introduction

The magnetorheological fluid (MRF) is a fluid composed of micron-sized metal particles suspended in a liquid such as silicone or hydrocarbon oil. The rheological properties of MRF rapidly and reversibly change under the influence of applying an external magnetic field. By applying the magnetic field, the suspended particles in the MRF are connected in a series of chains, limiting the fluid movement and thus increasing the yield stress of the fluid. MRF has Newtonian fluid behavior before applying the magnetic field (off state), but in the presence of a magnetic field (on the state), the rheological behavior of the fluid changes and it behaves similarly to the Bingham model fluid [1, 2]. In this model, the fluid behaves like a Newtonian fluid until it reaches the critical shear stress [3]. MRFs can be used to make various mechatronic devices [4-5]. In recent years, the design, modeling, and use of magnetorheological (MR) valves have been investigated by many researchers to develop MR dampers [6, 7]. In the MR electro-hydraulic activation systems, Olabi and Grunwald [9] studied two types of pressure controllers (the control valve and orifice control) with two types of MRF, one with a silicone base and the other with a hydrocarbon base. Goncalves and Carlson [10] presented a different valves model with an inclined cross-section and achieved better results than when did other types of valves. Gedik et al. [11] simulated and investigated the MRF flow velocity between two parallel plates under a magnetic field. Hung Nguyen et al. [1] found that the optimal design of MR valves was fundamental to minimize the energy consumption. They have also shown that the wire diameter has no significant effect on optimization and could be ignored. Wang et al. [12] examined MR valves with radial and annular fluid flow gaps under the magnetic flux. The obtained results by ANSYS software showed that the pressure drop in the annular-radial flow was more than that of the only annular flow and the central pressure drop in the radial flow showed that the simulation was well compatible with the experimental model. Hazem et al. [13] solved the magnetohydrodynamic (MHD) equation within a tube in the presence of a magnetic field. They concluded that the effect of changes in the magnetic field and viscosity was more significant than the Bingham number. Also, with the increasing magnetic field or yield stress, the flow rate decreased, and friction increased inversely. Yu and Warley [14] introduced a high-efficiency, non-moving valve. Kaluvan et al. [15] developed a new magnetorheological fluid actuator with desired control output. Brigadno et al. [16] provided fundamental relationships for the non-dense, non-Newtonian MRF. Koo et al. [17] found that it took about 25 milliseconds for an MR damper to reach 0.75 of the damping power. Milky et al. [18] used a phase voltage to activate rotary and linear MR dampers. The MR damper piston was moving at a constant speed, and when the voltage was off and on, the power of the damper was measured. It has been found that the response time of the damper varies between 30 and 180 milliseconds and is highly dependent on the voltage. Kavili Oglu et al. [19] examined the response time of a limited-slip differential (LSD) clutch control system in three different areas. The first zone is the interval between the “On” and “Off” states of the controller. The MRF LSD clutch is off in this interval, and The second zone is defined as the interval between the controller and the first MRF LSD clutch acceleration

point on the output shaft. The third zone is defined as the interval between the first acceleration point and the point at which the output shaft reaches a constant speed. They observed that the response time in all areas was a function of the input current and input speed. The response time decreases by increasing the speed and input current. It was found that when the partial volume fraction was kept constant in the MRF, the response time of the system, including the computer, controller, clutch, and MRF, varied between 20 and 65 milliseconds.

Therefore, according to the previous research [20, 21], this articles' main purpose is to investigate the feasibility of using magneto rheological valves in the oil and gas industry. In that regard, stable MRF was synthesized, and the rheological properties were examineated. Matlab fitted the Bingham model, and then that model data was used for the CFD Simulation of MR valve. Finally, the behavior of MRF in the Sleeve valve was simulated by Fluent Software.

2. Experimental

2.1. Magnetorheological fluid synthesis

MRF is generally synthesized through three phases: the continuous phase, dispersed particles, and stabilizer additives. The stable MRF used in this research, has been made by the method mentioned in the previous study [22-25], of which the details are brought in Table 1 briefly.

Table 1

Specification of the synthesized MRF sample.

Sample	Continuous phase (wt %)	Dispersed phase (wt %)	Additives (wt %)
MRF	Silicon oil (37)	Carbonyl iron (60)	Optimized value of stabilizer additives (3)

2.2. Viscosity measurement

Rheological properties are significant factors in MRF. In order to measure these properties, the inclined plate rheometer MCR300, Anton-Paar, Germany was used. The magnetorheological device MRD 180, Physica, Germany, under the uniform magnetic field was perpendicularly applied. Rheological properties containing the viscosity and shear stress of the stabilized MRF sample were measured at the constant temperature of 25 ^{o}C with different shear rates of 1000 - 0.0001 s^{-1}. The magnetic field was also set in the range of 2-0 A.

3. Modeling and simulation

3.1. Rheological modeling

The Bingham model was used for the evaluation of the rheological properties of MRF at the high shear rate. The viscosity and shear stress parameters were calculated by the minimal square weight linear method through MATLAB software. The results of the Bingham model parameters were used as the input data of CFD simulations. The Bingham plastic model is defined as:

$$\begin{cases} \tau = \tau_0 + \eta\gamma & \tau \geq \tau_0 \\ \gamma = 0 & \tau < \tau_0 \end{cases} \quad (1)$$

where τ, τ_0, γ , and η are the shear stress, yield stress, shear rate, and shear viscosity respectively.

3.2. CFD simulation equations

The substantial equations that govern simulation include continuity, momentum, and magnetization. The CFD technique can

be used to solve the mentioned equations numerically in the specific geometry, and thus the properties including speed, pressure, temperature, concentration and etc. are measured. This research involves continuity, Navier Stokes, and inducing equations defined as follows respectively.

3.2.1. Continuity equation

Eq. 2 shows the continuity equation for the incompressible fluid (is constant) that describes the transport of quantity.

$$\nabla . v = 0 \tag{2}$$

3.2.2. Momentum equation

The governing equation for the steady incompressible fluid in the magnetic field is:

$$\rho\left(\frac{\partial v}{\partial t} + (v.\nabla)v\right) = -\nabla P + \eta\Delta V + M \tag{3}$$

where is density, t the time, p the pressure, V the velocity vector, η is the viscosity, M the volumetric force (explained in part 3.2.3 and Nomenclature at the end of this paper).

3.2.3. Magnetization equation

Electromagnetic force (Lorentz force) applied to fluid from the magnetic field and performed as volumetric force (M) in momentum equations (3) calculated as per Eq. 4.

$$M = J \times B \tag{4}$$

J is the current density, and B represents the magnetic field flux in this equation. The current density of J is extracted from Ohm's law Eq. 12.

The magnetic field B is defined as Maxwell's equations. (Tesla) and (V/m) represent the magnetic and electric fields in these equations respectively. The induction field is determined by solving the below equations related to the electric field and the magnetic field. Furthermore, the electrical charge q (C/m^3) and current charge density (A/m^2) were calculated.

$$\vec{B} = 0 \tag{5}$$

$$\nabla \times \vec{E} = -\frac{\partial \vec{B}}{\partial t} \tag{6}$$

$$\nabla . \vec{D} = q \tag{7}$$

$$\nabla \times \vec{H} = \vec{j} \mp \frac{\partial \vec{D}}{\partial t} \tag{8}$$

Eq. 9 and Eq.10 show the induction fields and formulation.

$$\vec{H} = \frac{1}{\mu}\vec{B} \tag{9}$$

$$\vec{D} = \varepsilon\vec{E} \tag{10}$$

To investigate the interaction between the magnetic and electric fields, it is essential to know that current charge density affects the induction in two ways: solving the magnetic induction equation or solving the electric potential equation. In this study, the magnetic induction equation was used to calculate the current density.

3.2.4. Magnetic induction

The magnetic induction equation is derived from Ohm's law and Maxwell's equations. The obtained equation explained the relation between the magnetic and electric fields. In general, Eq. 11 defines Ohm's law that points to the relation between the current density and the electric field.

$$\vec{j} = \sigma(\vec{E} + \vec{v} \times \vec{B}) \tag{11}$$

In this equation, the constant coefficient is the electrical conduction. If the fluid is stationary, this general equation is simplified to Eq. 12.

$$\vec{j} = \sigma\vec{E} \quad (12)$$

The induction equation, finally derived from the combination of Maxwell's equations and Ohm's law, shows in Eq. 13.

$$\frac{\partial\vec{B}}{\partial t} + (\vec{v}.\nabla)\vec{B} = \frac{1}{\mu\sigma}\nabla^2\vec{B} + (\vec{B}.\nabla)\vec{v} \quad (13)$$

3.3. The geometry of CFD simulation

As it can be seen in Figure 1, the sleeve valve consists of a body and a flexible part (sleeve). MRF in the presence of the magnetic field was investigated based on the geometry provided in Figure 2 to evaluate the pressure decreasing at the sleeve. It must be mentioned that, due to observing changes in the MR pressure, a 2D geometry is provided as it can be seen in Figure 1.

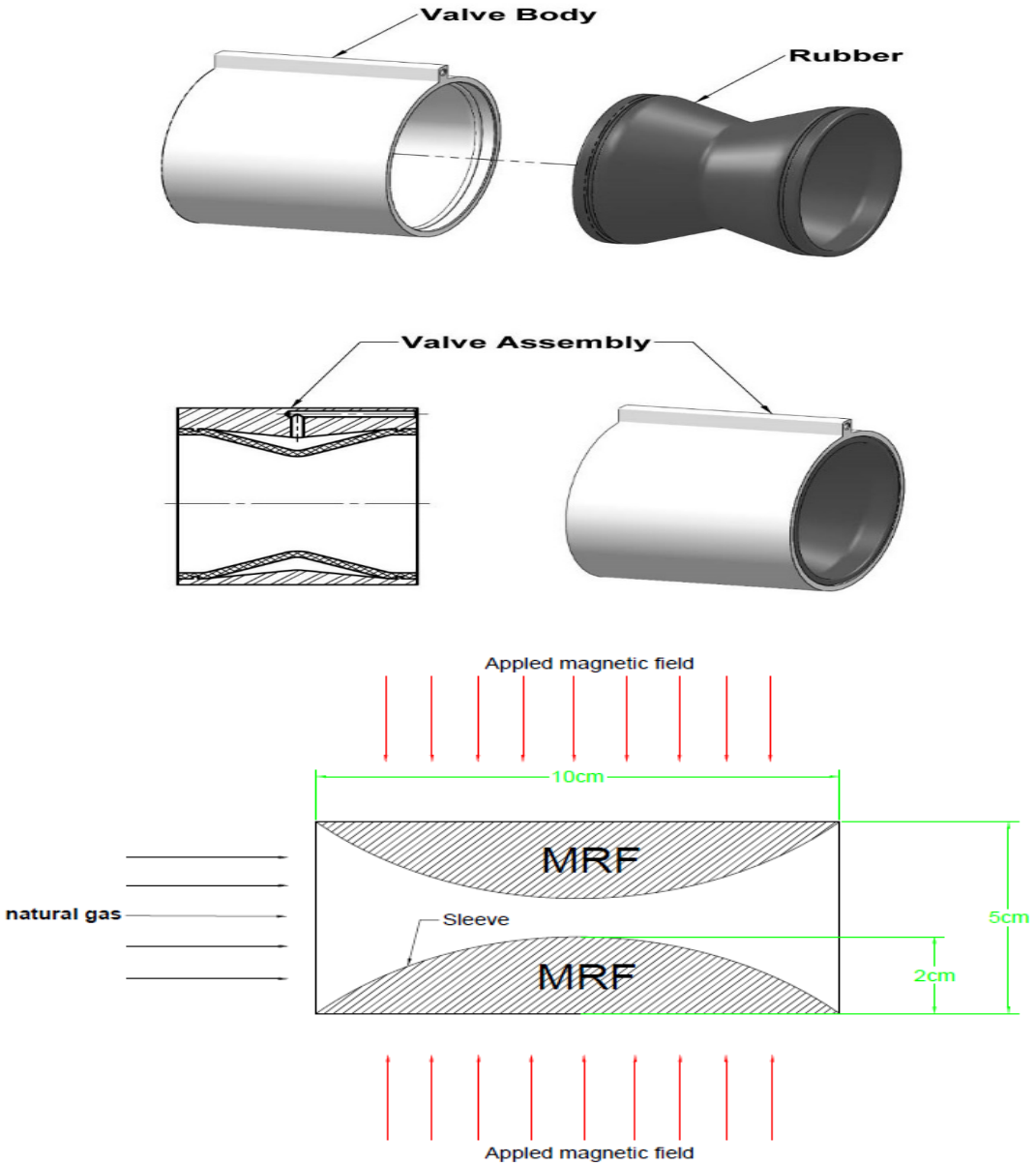

Figure 1. Sleeve valve components and the geometry of the MR valve for the CFD simulation.

4. Results and discussion

The result of the experimental measurements determined by the MCR300 device has been shown in Figure 2. The results reveal that the shear stress increases by applying an ascending magnetic field until it reaches the

magnetization saturation where the magnetic field does not affect the rheological properties and shear stress of MRF.

The Bingham model parameters interpolated from data are shown in Figure 2 to provide the input data to the simulation categorized in Table 2.

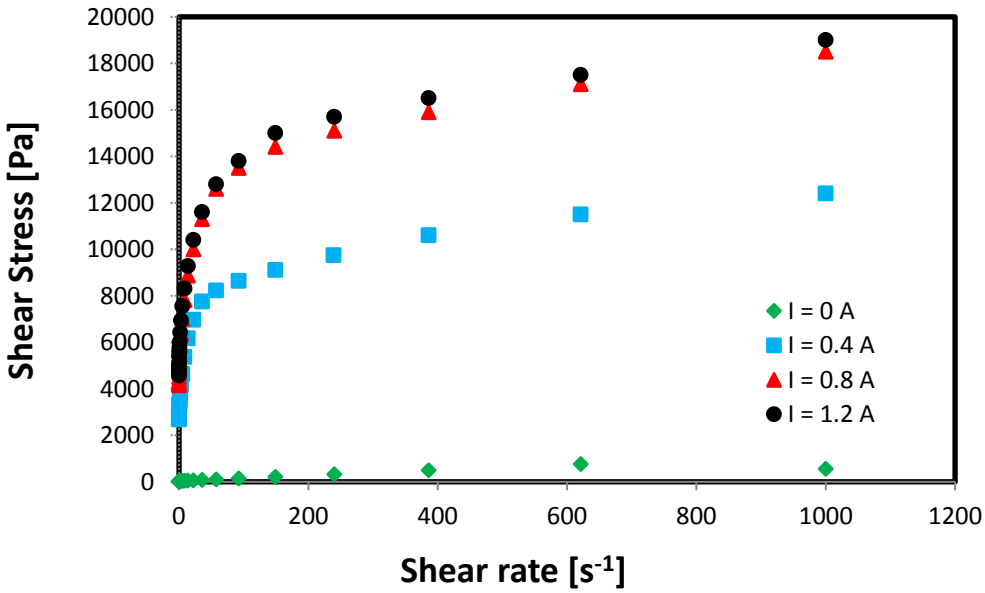

Figure 2. Experimental result of the magnetorheological fluid: The shear rate.

Table 2
Bingham model parameters obtained by MATLAB.

Parameter	H (A)			
	0	0.4	0.8	1.2
	81937	12600	24428	27132
μ	0.6827	0.6390	0.6410	0.6454
R*	0.9843	0.9754	0.9800	0.9794

*** The regression coefficient**

To select the appropriate mesh size in the presence of the magnetic field with a value of 0.5 Tesla, the amount of the applied pressure by MRF on the sleeve valve is measured in different mesh sizes. This procedure is repeatedly done through ANSYS Fluent 16.0 software by reducing the mesh size until the difference between the obtained pressures reaches below 1000 pascal (0.01 bar). In other words, the mesh size reduction continues to find the optimized and accurate size gained in the step where the difference between the pressures of the two respective cases is negligible. Therefore, the mesh number of 24670 is the most suitable one found by this method for the CFD simulation, as shown in Table 3.

The simulation was carried out for the sleeve valve geometry by MRF properties. The geometry of the industrial sleeve case was simulated by using the mesh with the optimal size (24670 elements no.) in the different magnetic fields altering between 1.5 and 0.2 Tesla. The contours resulted for five cases are shown in Figure 3.

Table 3

Obtained pressure with different mesh sizes.

No.	Mesh size (mm)	Element no.	Pressure (Pascal)
1	3	708	78812.54
2	2	1584	84003.48
3	1	6128	112223.13
4	0.5	24670	124584.80
5	0.25	99060	124903.22

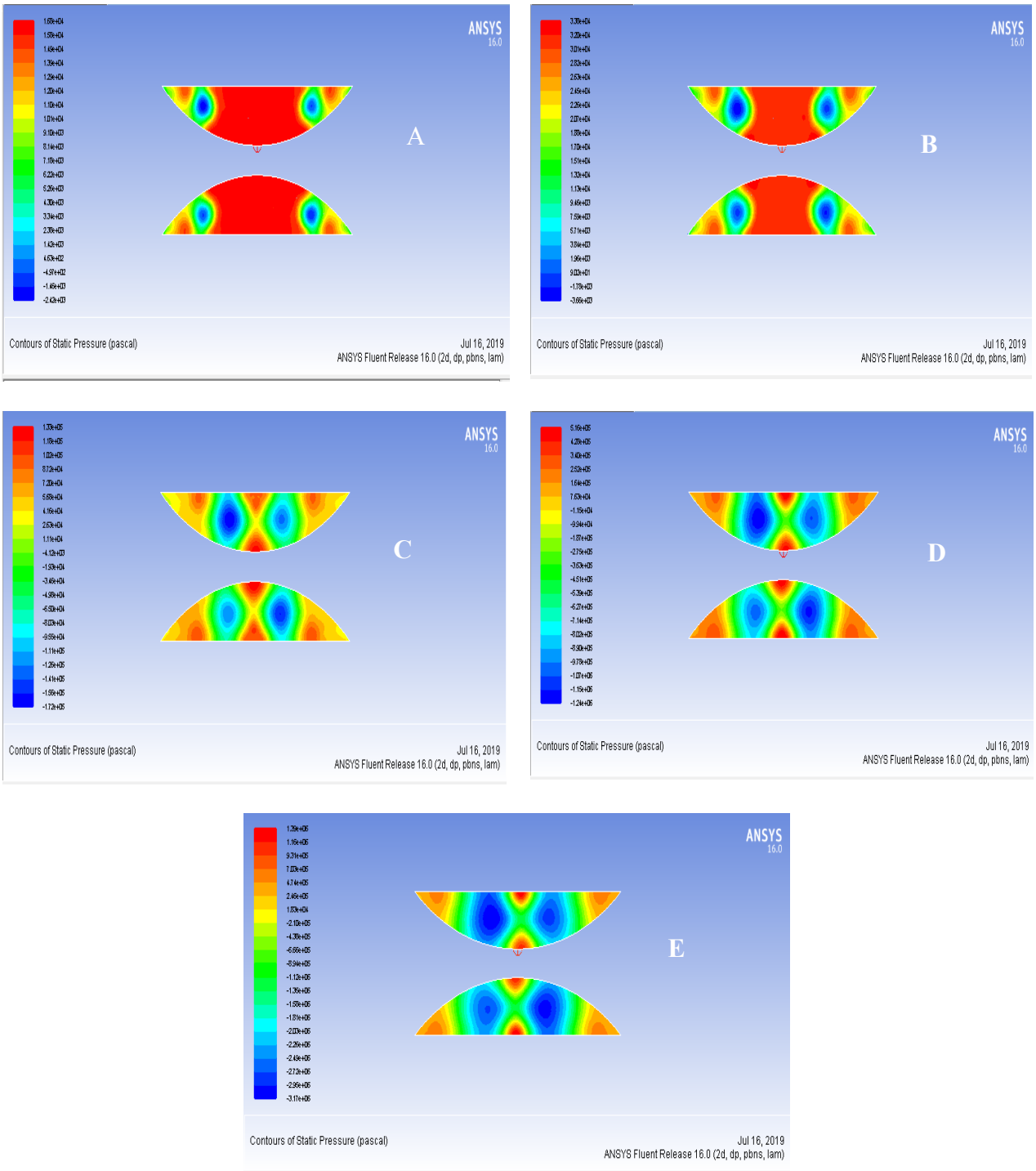

Figure 3. Pressure contour in different magnetic fields: (A) 0.2, (B) 0.3, (C) 0.5, (D) 1, and (E) 1.5 Tesla.

The pressure in the throat area of the valve was increased by increasing the magnetic field. Increasing pressure also affects the concentration of pressure in the valve throat.

Validating the MRF properties is a crucial point of this work. For this purpose, the MRF velocity between two parallel plates at the distance of 1 cm and the length of 30 cm was examined based on the Gedik et al. [11] research. In other words, the similar geometry of this refrence has been used to evaluate the MRF properties derived from experiments. The mentioned geometry was divided into three zones: the upstream of the flow, middle zone, and downstream of the stream, which is the field in the middle zone. After selecting the appropriate mesh size which was obtained according to the Gedik et al. [11] research, the simulation was carried out. Figure 4 shows the simulation result, which has the same trend as the data obtained from the Gedik et al. [11] research does, and the mean absolute erorr is 0.015 for this data. The fluid between the two plates is subjected to an input pressure of 500 Pascals and placed in different magnetic fields, and the obtained velocities are compared with each other. In the 1 and 1.5 Tesla of the magnetic field, the velocity values are 0.14 and 0.073 m/s respectively. The boundary conditions are 500 Pascal at the input, zero Pascal at the output, and the fluid behavior is in accordance with Bingham model. The fluid density, fluid viscosity, and magnetic permeability were considered 2380 kg/m^3, 0.042 kg/ms, and 4-7×10 h/m respectively.

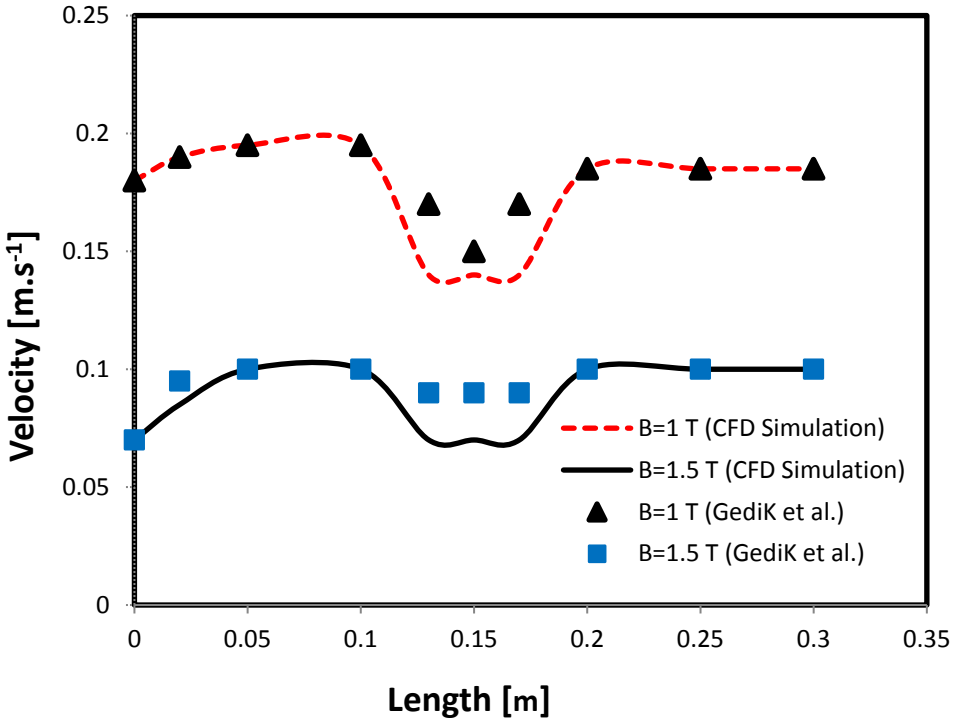

Figure 4. Validation of the CFD simulation with the Gedik et al. [11] research.

The pressure diagram and the value of the applied pressure in different magnetic fields indicate that increasing the magnetic field besides causing pressure to increase, centralizes the applied pressure to the sleeve throat; Figure 5. This centralization of the applied pressure makes the sleeve valve a proper choice for being investigated more.

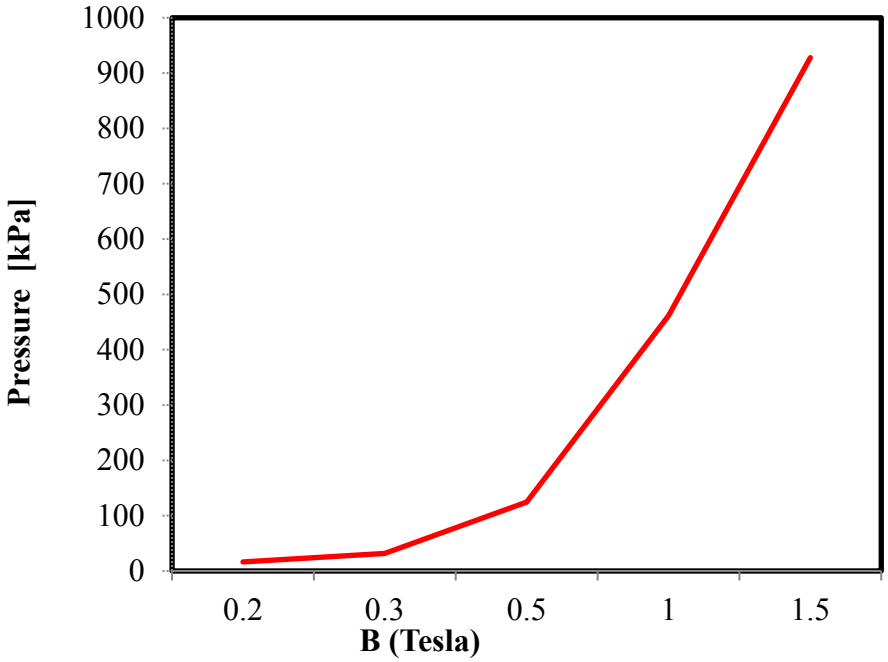

Figure 5. Applied pressure in the center of the sleeve throat by altering the magnetic field.

5. Conclusions

The MRF has been used in the sleeve valve to discover if it can actuate this special valve. At first, MRF was synthesized, and its properties were measured by MCR 300 rheometer. The Bingham model was used for the CFD simulation. In that connection, the model's coefficients were calculated based on the experimental results and MATLAB fitting. After finding the optimal mesh size, several simulations were carried out to see the trend of the applied pressure by MRF in the presence of different magnetic fields. The results showed that an increase in the magnetic field would cause an increase in the pressure at the sleeve's throat. The magnetic field of up to 0.5 Tesla, increases pressure and decreases amplitude. Therefore, as the magnetic field increased, the amplitude of the maximum pressure at the sleeve was significantly reduced. Furthermore, the pressure centralization increases in high magnetic fields. Although a quick response time in the presence of a magnetic field and the high controllability of MRF makes it an appropriate choice of being used in the control valve, the MRF application in the sleeve valve needs more investigation.

Acknowledgement

National Iranian Gas Company, Alborz Province Gas Company and PetroPars Operation and Management Company (POMC) are appreciated for their financial support and technical information.

Nomenclature

B	the magnetic flux density of the medium [Wb].
C_D	drag coefficient.
D	diameter of particle [m].
F	force of interaction between the continuous phase and dispersed phase [N].
F_D	drag force [N].
F_E	additional forces exerted on the particle [N].
g	gravity [m^2/s].
H	magnetic field intensity [T].

I	electrical current [A].
E	passing electrical current through wire [A].
p1	dipole moment of particle 1 [C.m].
p2	dipole moment of particle 2 [C.m].
P	pressure [Pa].
Re	Reynolds number for the continuous phase.
r	separation distance between the two dipoles [m].
T	temperature [K].
t	time [s].
V	velocity of the continuous fluid [m/s].
v	velocity of particle [m/s].

Greek symbols

μ_e	magnetic permeability [H/m].
μ	viscosity of the continuous phase [m^2/s].
ρ	density of the continuous fluid [Kg/m^3].
τ	shear stress of the continuous fluid [Pa].

References

[1] Nguyen, Q. H., Choi, S. B. and Wereley, N. M., "Optimal design of magnetorheological valves via a finite element method considering control energy and a time constant", *Smart Materials and Structures*, **17**, 025024 (2008).

[2] Rabbani, Y., Shirvani, M., Hashemabadi, S. H. and Keshavarz, M., "Application of artificial neural networks and support vector regression modeling in prediction of magnetorheological fluid rheometery", *Colloids and Surfaces A: Physicochemical and Engineering Aspects*, **520**, 268 (2017).

[3] Wang, D. H. and Liao, W. H.,"Magnetorheological fluid dampers: A review of parametric modelling", *Smart Materials and Structures,* **20**, 023001 (2011).

[4] Kordonsky, W., "Elements and devices based on magnetorheological effect", *Journal of Intelligent Material Systems and Structures,* **4**, 65 (1993).

[5] Carlson, J. D., Catanzarite, D. M. and Clair, K. A. S., "Commercial magneto-rheological fluid devices", *International Journal of Modern Physics B,* **10**, 2857 (1996).

[6] Hitchcock, G. H., Wang, X. and Gordaninejad, F., "A new bypass magnetorheological fluid damper", *Journal of Vibration and Acoustics, Transactions of the ASME,* **129**, 641 (2007).

[7] Nam, Y. J. and Park, M. K., "Performance evaluation of two different bypass-type MR shock dampers", *Journal of Intelligent Material Systems and Structures,* **18**, 707 (2007).

[8] John, S., Chaudhuri, A. and Wereley, N. M., "A magnetorheological actuation system: Test and model", *Smart Materials and Structures,* **17**, 025023 (2008).

[9] Olabi, A. G. and Grunwald, A., "Design and application of magneto-rheological fluid", *Materials and Design,* **28**, 2658 (2007).

[10] Goncalves, F. D. and Carlson, J. D., "An alternate operation mode for MRFs—magnetic gradient pinch", *Journal of Physics: Conference Series,* **149**, 012050 (2009).

[11] Gedik, E., Kurt, H., Recebli, Z. and Balan, C., "Two-dimensional CFD simulation of magnetorheological fluid between two fixed parallel plates applied external magnetic field", *Computers and Fluids,* **63**, 128 (2012).

[12] Wang, D. H., Ai, H. X. and Liao, W. H., "A magnetorheological valve with both annular and radial fluid flow resistance gaps", *Smart Materials and Structures,* **18**, 115001 (2009).

[13] Attia, H. A. and Ahmed, M. E. S.,

"Unsteady MHD flow in a circular pipe of a dusty non-Newtonian fluid", *Mechanics and Mechanical Engineering*, **11**, 113 (2007).

[14] Yoo, J. H. and Wereley, N. M., "Design of a high-efficiency magnetorheological valve", *Journal of Intelligent Material Systems and Structures,* **13**, 679 (2002).

[15] Kaluvan, S., Thirumavalavan, V., Kim, S. and Choi, S. B., "A new magneto-rheological fluid actuator with application to active motion control", *Sensors and Actuators, A: Physical,* **239**, 166 (2016).

[16] Brigadnov, I. A. and Dorfmann, A., "Mathematical modeling of magnetorheological fluids", *Continuum Mechanics and Thermodynamics*, **17**, 29 (2005).

[17] Koo, J. H., Goncalves, F. D. and Ahmadian, M., "A comprehensive analysis of the response time of MR dampers", *Smart Materials and Structures*, **15**, 351 (2006).

[18] Milecki, A., "Investigation of dynamic properties and control method influences on MRF dampers' performance", *Journal of Intelligent Material Systems and Structures*, **13**, 453 (2002).

[19] Kavlicoglu, N. C., Kavlicoglu, B. M., Liu, Y., Evrenesl, C. A., Fuchs, A., Korol, G. and Gordaninejad, F., "Response time and performance of a high-torque magneto-rheological fluid limited slip differential clutch", *Smart Materials and Structures,* **16**, 149 (2007).

[20] Maroofi, J., Hashemabadi, S. H. and Rabbani, Y., "Investigation of the chain formation effect on thermal conductivity of magnetorheological fluids", *Journal of Thermophysics and Heat Transfer,* **34** (1), 3(2020).

[21] Shirvani, M. and Rabbani, Y., "The properties and parameters needed of the magnetorheological fluid for use in the intelligent damper of the vehicle suspension system", *Nashrieh Shimi va Mohandesi Shimi Iran*, (2019).

[22] Rabbani, Y., Ashtiani, M. and Hashemabadi, S. H., "An experimental study on the effects of temperature and magnetic field strength on the magnetorheological fluid stability and MR effect", *Soft Matter*, **11**, 4453 (2015).

[23] Rabbani, Y., Hajinajaf, N. and Tavakoli, O., "An experimental study on stability and rheological properties of magnetorheological fluid using iron nanoparticle core–shell structured by cellulose", *Journal of Thermal Analysis and Calorimetry*, **135**, 1687 (2019).

[24] Rabbani, Y. and Tavakoli, O., "Experimental study on stability of magnetorheological fluid by using of Fe_3O_4/cellulose nanoparticles", *Amirkabir Journal of Mechanical Engineering*, **52** (10), 2779 (2019).

[25] Rabbani, Y., Shariaty Niassar, M. and Seyyed Ebrahimi, S. A., "An investigation of the effects of dopamine on the superhydrophobicity of carbonyl iron particles with stearic acid", *Iranian Journal of Chemical Engineering*, **17** (4), 49 (2020).